Proc. Natl. Acad. Sci. USA
Vol. 88, pp. 2702–2706, April 1991
Biochemistry

Intracellular distribution of microinjected antisense oligonucleotides

(diffusion/fluorescent oligonucleotides/nuclear location)

JEAN PAUL LEONETTI, NADIR MECHTI, GENEVIÈVE DEGOLS, CORINNE GAGNOR, AND BERNARD LEBLEU*

Laboratoire de Biochimie des Protéines, URA 1191 Centre National de la Recherche Scientifique, Université Montpellier II Sciences et Techniques du Languedoc, Place E. Bataillon C012, 34095 Montpellier Cedex 5, France

Communicated by Max L. Birnstiel, December 19, 1990

ABSTRACT **Antisense oligomers constitute an attractive class of specific tools for genetic analysis and for potential therapeutic applications. Targets with different cellular locations have been described, such as mRNA translation initiation sites, pre-mRNA splicing sites, or the genes themselves. However the mechanism(s) of action and the intracellular distribution of antisense oligomers remain poorly understood. Antisense oligomers conjugated with various fluorochromes or with BrdUrd were microinjected into the cytoplasm of somatic cells, and their cellular distribution was monitored by fluorescence microscopy in fixed and nonfixed cells. A fast translocation in the nuclei and a concentration on nuclear structures were observed whatever probe was used. Nuclear transport occurs by diffusion since it is not affected by depletion of the intracellular ATP pool, temperature, or excess unlabeled oligomer. Accumulation of the oligomers in the nuclei essentially takes place on a set of proteins preferentially extracted between 0.2 M and 0.4 M NaCl as revealed by crosslinking of photosensitive oligomers. The relationship between nuclear location of antisense oligomers and their mechanism of action remains to be ascertained and could be of major interest in the design of more efficient antisense molecules.**

The ability of antisense oligomers to interfere specifically with mRNAs or their precursors provides a valuable tool for the control of cellular and viral gene expression (for review, see ref. 1). Although attractive, this approach is restricted by the poor stability of natural oligomers and the low efficiency of their cellular uptake. These difficulties can at least be partially circumvented by the use of nuclease-resistant analogs or drug delivery techniques (2). Despite these advances, the design of optimal strategies for oligomer synthesis and delivery has remained difficult since not much is known about the mechanism through which antisense oligomers interfere with gene expression within intact cells or of their intracellular fate.

The antisense concept is based on the assumption that complementary DNA or RNA sequences might interact with mRNA to block their translation. To overcome the complexity of investigation in intact cells, several laboratories have developed cell-free models to evaluate the inhibitory potential of these molecules. Nevertheless, cell-free studies have usually been limited to observations at the translational level and are not always representative of the intact cell situation. Antisense oligomers were successfully used on cultured cells against various targets, such as translation initiation (3), introns (4), and splice sites (5). The subcellular locations of these targets lead to the assumption that oligomers might act in the cytoplasm and/or the nuclei.

Charged oligomers are internalized through an endocytic pathway (6, 7), and a punctuated cytoplasmic labeling characteristic of accumulation in the endocytic vesicles is indeed observed when fluorescently tagged oligomers are used (6). However other reports have described a preferential nuclear location of these oligomers (8, 9). We therefore tried to ascertain the fate and the intracellular location of small antisense oligomers directly introduced by microinjection in the cytoplasm of somatic cells.

MATERIALS AND METHODS

Oligomer Synthesis and Nomenclature. Oligomer 1 (CATTTTGATTACTGT), complementary to the 5′ end sequence of vesicular stomatitis virus N protein mRNA, and oligomer 2, initially designed to hybridize through triple helix formation on the murine c-*myc* oncogene ($U^{Br}C^{Me}U^{Br}C^{Me}U^{Br}C^{Me}C^{Me}C^{Me}C^{Me}U^{Br}U^{Br}U^{Br}T$), were synthesized using an automatic synthesizer and the phosphoramidate method. The phosphorothioate oligomer 3 (CATTTTGATTACTGT) was synthesized using the hydrogen phosphonate method and oxidized according to the manufacturer's instructions.

Oligomer Modification. The 5′ end of detritylated oligomers (uncleaved from synthesis support) was activated with carbonyldiimidazole and modified with diaminohexane according to ref. 10. After cleavage from the column and deprotection, the oligomers were labeled with fluorescein isothiocyanate (FITC) or tetramethylrhodamine isothiocyanate (TRITC) (in 50-fold excess compared to the oligomer) in 20 mM triethylammonium acetate, pH 8/30% (vol/vol) dimethylformamide for 2 hr. Free fluorescent dye was removed by serial ethanol precipitations followed by reversed-phase HPLC.

Protein Labeling and Conjugation. Bovine serum albumin (BSA; 20 mg) was incubated with TRITC (0.5 mg) in 100 mM triethylammonium acetate (pH 8) for 2 hr. Free dye was then removed by gel filtration on Sephadex G-50. The synthetic peptide Cys-Gly-Tyr-Gly-Pro-Lys-Lys-Lys-Arg-Lys-Val-Gly-Gly including the 7-amino acid core sequence required for simian virus 40 (SV40) T antigen nuclear transport (containing 1:10 ^{125}I-iodinated peptide), was conjugated to TRITC-labeled BSA using the heterobifunctional reagent *m*-maleimidobenzoyl-*N*-hydroxysuccinimide ester (Pierce) according to ref. 11. The conjugates were analyzed by SDS/PAGE (12) and autoradiography.

Cell Culture and Microinjection. Rat embryo fibroblasts REF-52 were grown on plastic culture dishes in Dulbecco's modified Eagle's medium complemented by 10% (vol/vol) fetal calf serum. Glass needles were stretched with a Leitz horizontal puller, and microinjections ($\approx 5 \times 10^{-14}$ liter per cell) were performed with a Leitz manual micromanipulator under fluorescent or phase-contrast microscopy. BSA con-

The publication costs of this article were defrayed in part by page charge payment. This article must therefore be hereby marked "*advertisement*" in accordance with 18 U.S.C. §1734 solely to indicate this fact.

Abbreviations: AMCA, 7-aminomethylcoumarin hydroxysuccinimide ester; BSA, bovine serum albumin; FITC, fluorescein isothiocyanate; SV40, simian virus 40; TRITC, tetramethylrhodamine isothiocyanate.

*To whom reprint requests should be addressed.

jugates (10 mg/ml) or oligomers (200 μg/ml; 10^6 molecules per cell) in distilled water were injected alone or coinjected with FITC-labeled dextran (M_r 70,000; 2 mg/ml). Usually 20–50 cells were injected in each experiment and the data were reproduced at least three times. After microinjection, the cells were incubated at 37°C, fixed 5 min in ethanol/30% (vol/vol) acetone, mounted in 0.1 M Tris, pH 8.5/0.1 mg of moviol 488 per ml/25% (vol/vol) glycerol, and photographed using an Axiophot Zeiss photomicroscope and Kodak Tmax 3200 films unless otherwise specified.

Nuclear Protein Extraction. Nuclei from REF-52 cells were prepared as described (13). After cell lysis, the homogenate was centrifuged for 10 min at 2000 rpm in a Sorvall HG4L rotor. The supernatant containing the cytoplasmic fraction was recovered according to ref. 13 and frozen at −80°C. An aliquot of the nuclear pellet was resuspended in 1 ml of storage buffer [20 mM Hepes, pH 7.9/20% (vol/vol) glycerol/0.1 M KCl/0.2 mM EDTA/0.5 mM phenylmethylsulfonyl fluoride (PMSF)/0.5 mM dithiothreitol] and was frozen. Nuclear proteins were first extracted from the pellet with buffer C [20 mM Hepes, pH 7.9/25% (vol/vol) glycerol/1.5 mM $MgCl_2$/0.2 mM EDTA/0.5 mM PMSF/0.5 mM dithiothreitol/0.05 M NaCl]. After centrifugation, the resulting pellet was further extracted with buffer C/0.2 M NaCl and later extracted with buffer C/0.4 M NaCl. To recover histones, the remaining pellet was resuspended in 50 μl of 0.1 M HCl/0.5% (vol/vol) Triton X-100 and incubated for 10 min on ice. After dilution to 0.3 ml with distilled water and centrifugation at 25,000 × *g* for 10 min, the supernatant was recovered. The nuclear extracts were then dialyzed against 50 vol of storage buffer, adjusted to the same protein concentration, and frozen at −80°C.

Photolabeling of Proteins with Radioactive Oligomers. The photosensitive oligomer containing BrdUrd was 5′ labeled with [α-^{32}P]ATP and polynucleotide kinase; 10^5 cpm were incubated with nuclei and nuclear or cytoplasmic extracts (10 μg of protein in 0.3 ml of phosphate-buffered saline). After UV irradiation (40 min under a Philips HPLK 400-W bulb) proteins were precipitated at −20°C with 5 vol of acetone, using 20 μg of BSA as carrier, and fractionated by SDS/PAGE (14) (12.5% wt/vol). Proteins crosslinked to the oligomers were revealed by autoradiography with Kodak X-Omat films in the presence of intensifying screens.

RESULTS

Subcellular Distribution of Synthetic Oligomers. In most of the experiments described here, 15-mer oligomers with regular phosphodiester linkages (oligomer 1) and in some cases phosphorothioate derivatives (oligomer 3) were used (see *Materials and Methods* for sequences). Such oligomers were conjugated at their 5′ ends to FITC, TRITC, or 7-aminomethylcoumarin hydroxysuccinimide ester (AMCA) and microinjected into the cytoplasm of rat embryo fibroblasts (REF-52).

As shown in Fig. 1 *A* and *C*, most of the fluorescence was found to be associated with cell nuclei 30 min after microinjection of TRITC-labeled oligomer 1. The integrity of nuclear membranes was checked by coinjection of high molecular weight FITC-labeled dextran (M_r 70,000), which cannot diffuse freely through nuclear pores. As shown in Fig. 1*B*, microinjection does not induce passage of FITC-labeled dextran through the nuclear membrane.

Similar results were obtained with FITC- or AMCA-labeled oligomers (not shown). Unreactive free TRITC did not accumulate in the nucleus of microinjected cells and could almost totally be removed by fixation with organic solvents. The results obtained with fluorescently tagged oligomers are in line with another set of experiments performed with BrdUrd-modified oligomers, whose nuclear distribution was monitored by indirect immunofluorecence with BrdUrd-specific antibodies (not shown). These concordant results rule out any involvement of the dye in the nuclear translocation process. Other fixation procedures, such as microwave (14) and the direct monitoring of oligomer distribution in living cells, led to similar observations (not shown).

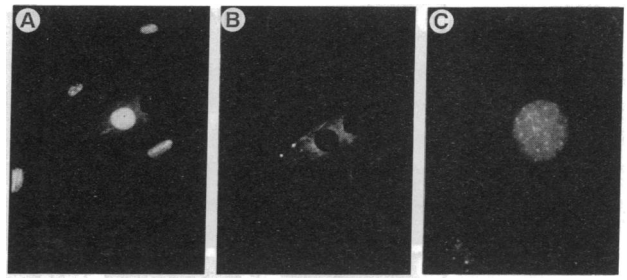

FIG. 1. Nuclear accumulation of rhodamine-labeled oligomers. TRITC-conjugated oligomer 1 (100 μg/ml) was coinjected with 2 mg of FITC-labeled dextran per ml (M_r 70,000) in the cytoplasm of REF-52 cells (see text for details of the conjugation and microinjection procedure). Cells were incubated for 30 min at 37°C and fixed with ethanol/acetone 70:30 (vol/vol). (*A* and *B*) Fluorescence photomicrographs (560× enlargement) display the same field. (*A*) TRITC-labeled material. (*B*) FITC-labeled material. (*C*) Detail of *A*.

To exclude the role of a particular cellular context in these experiments, microinjections were also performed in HeLa cells and Ltk$^-$ cells; they led to comparable patterns (not shown). No significant differences in the nucleo–cytoplasmic partition were observed whatever the oligomer sequences (various sequences were tested) or length (within a 15- to 50-mer range in our experiments) (not shown). Similar data have also been obtained with double-stranded oligomers of various lengths (not shown) or 2′-*O*-methylated ribonucleotide analogs used with a view to interfere with splicing events (A. Lammond, European Molecular Biology Laboratory Heidelberg, personal communication).

Kinetics of Oligomer Accumulation in Nuclei. Although the transfer of oligomers to the nucleus seemed to occur quite quickly, a precise evaluation of its kinetics was limited by the time required for cell fixation. Similar experiments were thus performed under inverted fluorescent microscopy on living cells. This allows a direct monitoring of intracellular fluorescence distribution in nonfixed microinjected cells and eliminates artefacts possibly linked to material redistribution during cell fixation. As shown in Fig. 2 *Lower*, FITC-tagged oligomers accumulated very rapidly in nucleus, with translocation being nearly completed by 1 min after microinjection. A similar experiment (Fig. 2 *Upper*) performed with a 10-fold excess of unlabeled oligomers with the same base composition did not affect the nuclear translocation of the fluorescent material. The small differences observed between Fig. 2 *Lower* and *Upper* cannot be considered as significant in our experimental conditions. In fixed cells, FITC-labeled dextran remained confined to the cytoplasm (not shown).

Possible Mechanism(s) of Oligomer Nuclear Translocation. Charged material, with the molecular mass range of the oligomers used throughout, could in principle diffuse freely through the nuclear pores. The following experiments were designed as the first steps toward distinguishing between diffusion, facilitated diffusion, and active transport of oligomers through the nuclear membrane.

A depletion of the intracellular ATP pool with 50 mM deoxyglucose and 5 mM NaN_3 (as verified by an ATP bioluminescence luciferin/luciferase assay; data not shown) did not significantly affect oligomer transport (Fig. 3*C*); this is generally considered as an argument for passive transport. Likewise, the rate of transport was unaffected when cells

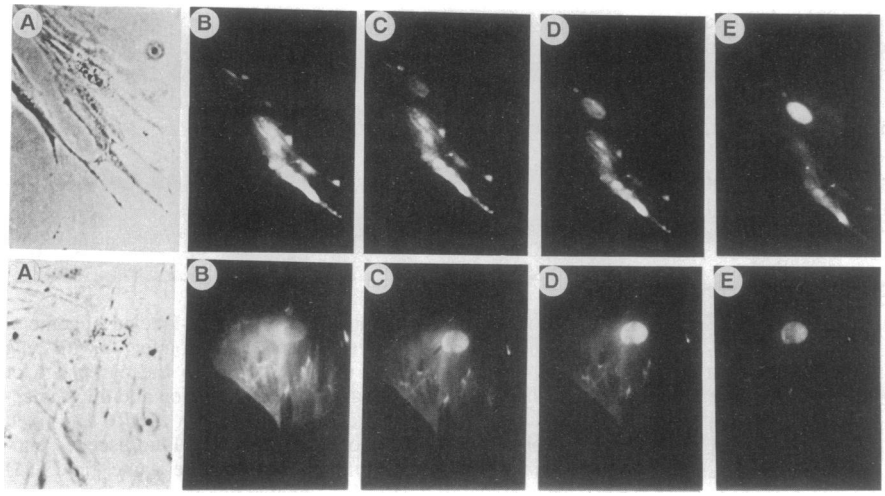

FIG. 2. Kinetics of nuclear uptake of FITC-labeled oligomers. FITC-conjugated oligomer 1 (200 μg/ml) was injected in the cytoplasm of REF-52 cells with (*Upper*) or without (*Lower*) a 10-fold excess of an unlabeled oligomer with the same sequence. Phase-contrast (*A*) or fluorescence (*B–E*) photomicrographs (700× enlargement) of the same microinjected cell are shown. The distribution of FITC-modified oligomer was analyzed on living cells 15 sec (*B*), 30 sec (*C*), 45 sec (*D*), and 60 sec (*E*) after microinjection.

were incubated at 4°C instead of 37°C (Fig. 3*B*). On the contrary, the transport of microinjected BSA–TRITC–peptide (a TRITC-labeled conjugate of BSA and of the SV40 karyophilic motif), used as a control of active nuclear transport, was totally inhibited by incubation at 4°C or by ATP depletion (Fig. 3), in keeping with published data (15).

Stability of Oligomers in the Nuclei. Degradation of oligomers is one of the major problems encountered in their use; we have thus determined the degree of stability with which oligomers become associated with nuclei. It is clearly evident that fluorescence remains at a maximum level for a relatively short period of time and decreases thereafter, to become undetectable 6–10 hr later. The latter phenomenon could reflect oligomer degradation. This point is illustrated in Fig. 4, where cells were coinjected with the FITC-labeled phosphodiester oligomer 1 and the nuclease-resistant (16) phosphorothioate oligomer 3 conjugated to TRITC and followed over a 20-hr period for both fluorochromes. The longer retention of nuclear fluorescence with the phosphorothioate is correlated with its increased metabolic stability, in keeping with the nuclear accumulation of the fluorochrome, this being a consequence of the oligomer integrity. In the same way, metabolically stable oligomers in the α-anomeric configuration (17) migrated rapidly to the nucleus and remained stably associated therein for long periods of time (not shown).

Sites of Oligomer Nuclear Accumulation. Whatever the details of the mechanism involved in oligomer uptake, the large accumulation of nuclear material implies the existence of nuclear binding sites. Interestingly, nuclei were not labeled homogeneously whether FITC or TRITC was used (Fig. 1*C*); this stippled pattern could reflect the distribution of nuclear binding sites.

As a first step toward identifying oligomer binding sites, nuclei were prepared by hypotonic lysis procedure known to maintain their integrity to the utmost. It was verified (data not shown) that the uptake of TRITC-labeled oligomers within such nuclei occurred with the same characteristics as those described above for microinjected cells.

In the experiments shown in Fig. 5, isolated nuclei were incubated with photosensitive ^{32}P-labeled oligomer deriva-

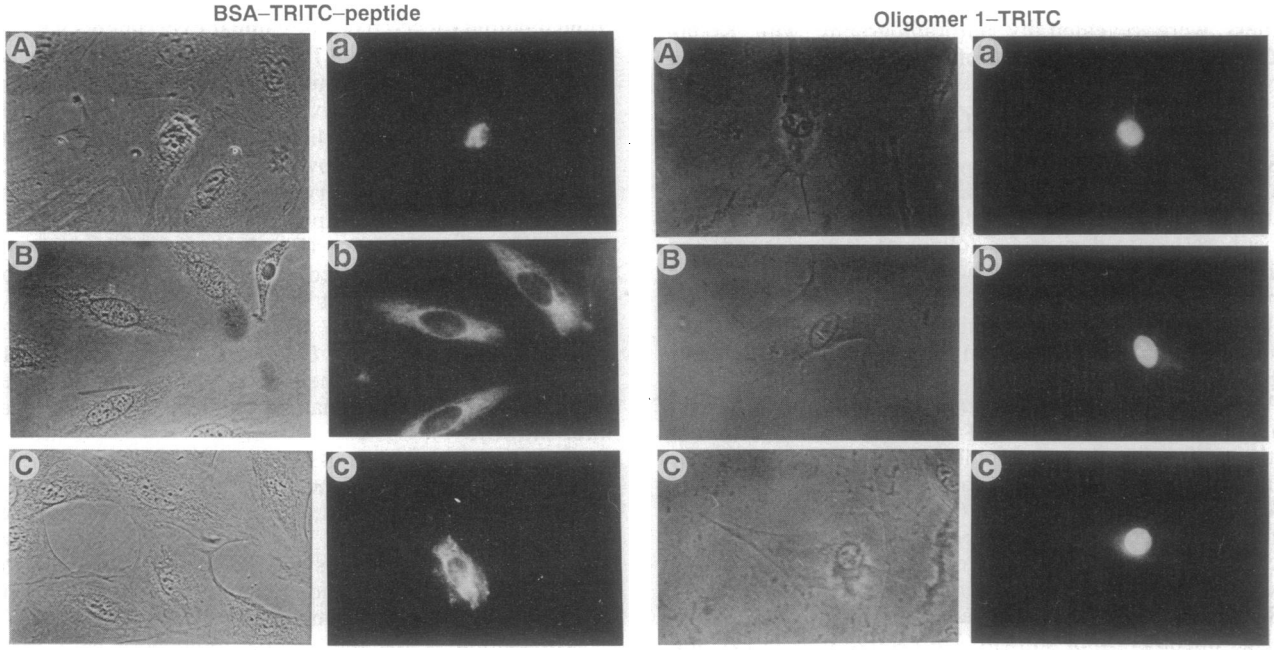

FIG. 3. Mechanism of nuclear transport of oligomers. TRITC-conjugated oligomer 1 (*Right*) and the BSA–TRITC–peptide (*Left*) were injected in REF-52 cell cytoplasm at 37°C (*A* and *a*), at 0°C (*B* and *b*), or at 37°C in the presence of 5 mM NaN_3 and 50 mM deoxyglucose (*C* and *c*). Fluorescence (*a–c*) or phase-contrast (*A–C*) photomicrographs (700× enlargement) taken from cells fixed 30 sec for oligomer 1-TRITC or 30 min for BSA–TRITC–peptide after microinjection are shown. The enlargement factor is 40-fold for oligomer 1-TRITC and 60-fold for BSA–TRITC–peptide.

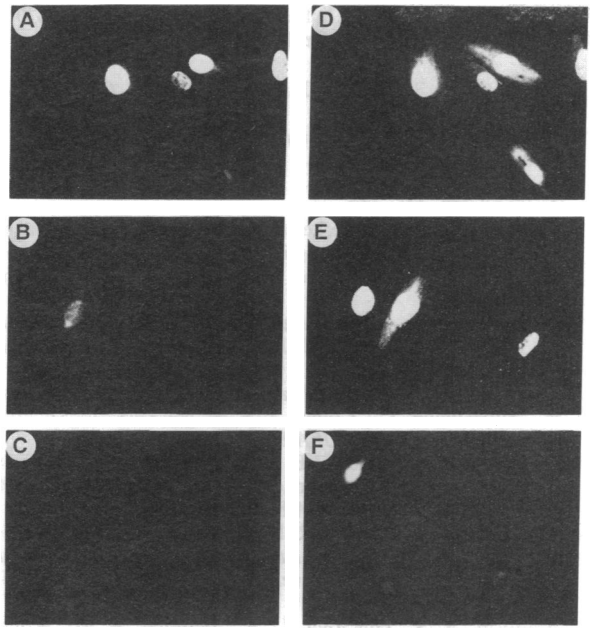

FIG. 4. Stability of the association of oligomers with the nucleus. REF-52 cells were coinjected with FITC-conjugated oligomer 1 (phosphodiester linkages) and TRITC-labeled oligomer 2 (phosphorothioate linkages), each at 100 μg/ml. Cells were fixed after 30 min (*A* and *D*), 3 hr (*B* and *E*), or 20 hr (*C* and *F*) of incubation at 37°C. Fluorescence photomicrographs (500× enlargement) reveal FITC- (*A–C*) or TRITC-labeled (*D–F*) material in the same cells.

tives and crosslinked by UV irradiation. A set of protein bands ranging essentially from M_r 36,000 to 50,000 was reproducibly labeled (Fig. 5, lane 2); little labeling of cytoplasmic proteins was obtained (Fig. 5, lane 7).

The binding of these photosensitive oligomers to nuclear proteins was competitively inhibited by an excess of unlabeled oligomers or by polyanions such as heparin (data not shown). These experiments were also attempted in microinjected cells; however the nuclear introduction of large amounts of polyanionic competitors turned out to be too cytotoxic to draw meaningful conclusions. As expected, electrostatic interactions appear to play a major role in the binding of oligomers to their nuclear receptors. Interestingly,

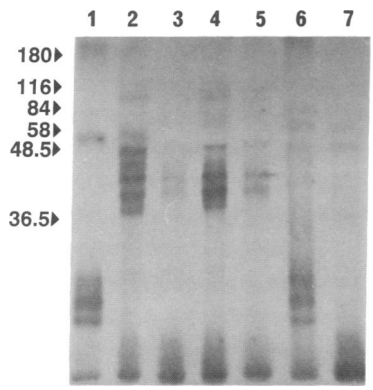

FIG. 5. SDS/PAGE analysis of oligomer-labeled proteins in intact nuclei and in nuclear extracts. Purified histones (lane 1), crude nuclei (lane 2), nuclear extracts prepared by treatment of crude nuclei with NaCl at 0.05 M (lane 3), 0.2 M (lane 4), and 0.4 M (lane 5) or by extraction with 0.01 M HCl/0.5% (vol/vol) Triton X-100 (lane 6), and cell cytoplasm (lane 7) were incubated with the ^{32}P-labeled photosensitive oligomer 3 and crosslinked by UV irradiation. Labeled proteins were fractionated by SDS/PAGE and the distribution of radioactivity was analyzed by autoradiography. Molecular weights are given as $M_r \times 10^{-3}$.

however, binding within intact nuclei did not take place significantly at the histone level (compare Fig. 5, lane 1 and lane 2). Sequential extraction of nuclear proteins at increasing ionic strength (Fig. 5, lane 3–5) or at acidic pH (Fig. 5, lane 6) followed by crosslinking with the photosensitive oligomer indicates that the 0.2 M NaCl fraction is the richest in oligomer binding sites. Histones were of course labeled when extracted from the nuclei (Fig. 5, lane 6) but were not labeled in their native environment (Fig. 5, lane 2).

DISCUSSION

The key finding of the present study is the rapid and preferential accumulation of microinjected small oligomers in the nucleus of intact cells. A punctated nuclear location was observed using various methods of detection, including fluorescence of FITC-, TRITC-, or AMCA-labeled oligomer, and immunodetection of BrdUrd-modified oligomers. Furthermore, fluorescently tagged phosphorothioates and α-oligomers, two analogs resistant to nuclease degradation, exhibited the same rapid nuclear location but could be detected even 20 hr after microinjection, whereas the fluorescence of unmodified oligomers disappeared within 3 hr. These converging results and the detection of fluorescence in the nuclei within a few seconds after microinjection exclude a nuclear location induced by the fluorochromes or the migration of the free dyes to the nucleus after degradation of the oligomer.

It was also verified that microinjection by itself did not induce damage to the nuclear membrane. In our experimental conditions, high molecular weight molecules (FITC-labeled dextran, M_r 70,000) that are not diffusible through the nuclear pore membrane remained in the cytoplasm of the cells when coinjected with the oligomers.

Two mechanisms of passage through the nuclear membrane have been reported: the active passage of large proteins containing a nuclear location signal (review in ref. 15) and the passive diffusion of small molecules (18, 19). In our experiments, the nuclear concentration of injected oligomers was unaffected by low temperature or ATP depletion, whereas at the same time the BSA–TRITC–peptide used as a control of nuclear active transport remained cytoplasmic. Furthermore, the coinjection of TRITC-labeled oligomer and of an excess of unlabeled oligomer did not significantly affect oligomer location. The independence with respect to temperature, ATP depletion, and competition with unlabeled molecules provides arguments in favor of a diffusion process, compatible with the small size of the oligomer. However these data are not sufficient to explain a nuclear accumulation, unless diffusion is followed by nuclear binding. Similar observations have recently been reported with small nonnuclear basic or acidic proteins (lysozyme, soybean trypsin inhibitor, cytochrome *c*), which accumulate in the nucleus of injected cells presumably after diffusion and nonspecific binding (19); this import mechanism was called the "diffuse and bind model" (15).

To investigate potential oligomer binding sites, photosensitive radioactively labeled oligomers were incubated with isolated nuclei and nuclear extracts. Four major bands ranging from M_r 36,000 to 50,000 were observed in intact nuclei, whereas only two of them could be detected in nuclear extracts. Possible explanations are (*i*) that proteins exhibit different conformations or complexation with nucleic acids or proteins in nuclei and in nuclear extracts and (*ii*) that some proteins cannot be extracted from nuclei in our experimental conditions. Oligomer binding to these proteins could be in competition with an unlabeled oligomer of the same sequence, with an unrelated one, or with heparin, a sulfated polyanion. The negative charges of the oligomers thus seem to be involved in these interactions. However histones did

not bind oligomers in intact nuclei, despite their abundance and cationic charges. The absence of competition for nuclear import in microinjected cells is apparently contradictory with the inhibition of oligomer binding in the presence of an excess of unlabeled oligomer or heparin on purified nuclei or nuclear extracts. However the nuclear targets might be highly expressed proteins. Moreover microinjection of high heparin or oligomer concentrations necessary for competition in intact cells was limited by cytotoxicity and precipitation problems.

A few reports have described the involvement of cytoplasmic factors in the nuclear import of proteins (20, 21). This is probably not the case with small oligomers since direct binding of these molecules took place in nuclei and nuclear extracts but not on cytoplasmic fractions; likewise, no competition with nonfluorescent oligomers for nuclear import could be achieved.

Present data provide interesting prospects for the study of the antisense oligomer mechanism of action. If microinjection really mimics the steps following oligomer escape from the endocytic pathway, the relation between nuclear location and mechanism of action needs to be elucidated. Nuclear sequences such as pre-mRNA splicing sites, exons, or genes themselves could be more interesting targets for synthetic oligomers than mature cytoplasmic mRNAs. However if a weak association of oligomers with nuclear structures potentially allows exchange between the binding proteins described above and the nucleic acid targets being sought, a strong nonspecific binding would be unfavorable to oligomer activity. Furthermore, although various data have demonstrated the biological activity of antisense oligomers specifically directed to nuclear targets, our data (22) and results from ref. 5 describe the antisense activity of modified oligomers directed to vesicular stomatitis virus, a virus with a replication cycle restricted to the cytoplasm. The mechanism of action of antisense oligomers is therefore probably not unique. Modifications allowing a cytoplasmic location of the oligomers and the measurement of their inhibitory activity as compared to unmodified ones could provide interesting information for the development of more efficient molecules.

We are grateful to Dr. J. C. Bonnafoux for his advice on peptide iodination and conjugation and to Prof. J. L. Imbach for the gift of FITC-labeled α-oligomers. J.P.L. and G.D. hold fellowships from the Ligue Nationale Francaise Contre le Cancer and the Association pour la Recherche contre le Cancer. This work was supported by grants from the Association pour la Recherche contre le Cancer, the Institut National de la Santé et la Recherche Médicale (CRE 881015), and the Centre National de la Recherche Scientifique.

1. Hélène, C. & Toulmé, J. J. (1990) *Biochem. Biophys. Acta* **1049**, 99–125.
2. Goodchild, J. (1990) *Bioconjugate Chem.* **1**, 165–187.
3. Heikkila, R., Schwab, G., Wickstrom, E., Loke, L. S., Pluznik, D. H., Watt, R. & Neckers, L. M. (1987) *Nature (London)* **328**, 445–449.
4. McManaway, M. E., Neckers, L. M., Loke, L. S., Al-Naeser, A. A., Redner, R. I., Shiramizo, B. T., Goldschmidts, W. I., Huber, B. E., Bhatia, K. & Magrath, I. T. (1990) *Lancet* **i**, 808–810.
5. Kulka, M., Smith, C. C., Aurelian, L., Fishelevich, R., Meade, K., Miller, P. & Ts'o, P. O. P. (1989) *Proc. Natl. Acad. Sci. USA* **86**, 6868–6872.
6. Loke, S. L., Stein, C. A., Zhang, X. H., Mori, K., Nakanishi, M., Subasinghe, C., Cohen, J. S. & Neckers, L. M. (1989) *Proc. Natl. Acad. Sci. USA* **86**, 3474–3478.
7. Yakubov, L. A., Deeva, E. A., Zarytova, V. F., Ivanova, E. M., Ryte, A. S., Yurchenko, L. V. & Vlassov, V. V. (1989) *Proc. Natl. Acad. Sci. USA* **86**, 6454–6458.
8. Goodchild, J., Lestsinger, R. L., Sarin, P. S., Zamecnik, M. & Zamecnik, P. C. (1988) in *Human Retroviruses, Cancer and AIDS: Approaches to Prevention and Therapy* (Liss, New York), pp. 423–438.
9. Boutorin, A. S., Gus'lova, L. V., Ivanova, E. M., Kobetz, N. D., Zarytova, V. F., Ryte, A. S., Yurchenko, L. V. & Vlassov, V. V. (1989) *FEBS* **254**, 129–132.
10. Wachter, L., Jablonski, J. A & Ramachandran, K. L. (1986) *Nucleic Acids Res.* **14**, 7985–7994.
11. Godfarb, D. S., Gariépy, J., Schoolnik, G. & Kornberg, R. D. (1986) *Nature (London)* **14**, 641–644.
12. Laemmli, U. K. (1970) *Nature (London)* **227**, 680–685.
13. Dignam, J. D., Lebowitz, R. M. & Roeder, R. D. (1983) *Nucleic Acids Res.* **11**, 1475–1489.
14. Barnosy, J. & Marx, S. J. (1990) *Proc. Natl. Acad. Sci. USA* **87**, 1188–1192.
15. Dingwall, C. & Laskey, R. A. (1986) *Annu. Rev. Cell. Biol.* **2**, 67–90.
16. Eckstein, F. (1985) *Annu. Rev. Biochem.* **54**, 367–402.
17. Thenet, S., Morvan, F., Bertrand, J. R., Gautie, C. & Malvy, C. (1988) *Biochimie* **70**, 1729–1732.
18. Lang, I., Scholz, M. & Peters, R. (1986) *J. Cell. Biol.* **102**, 1183–1190.
19. Breeuwer, C. & Goldfard, D. S. (1990) *Cell* **60**, 999–1008.
20. Baeuerle, P. A. & Baltimore, D. (1988) *Science* **242**, 540–546.
21. Picard, D., Salser, S. J. & Yamamoto, K. R. (1988) *Cell* **54**, 1073–1080.
22. Lemaitre, M., Bayard, B. & Lebleu, B. (1987) *Proc. Natl. Acad. Sci. USA* **84**, 648–652.